Specific Photoaffinity-Labeling of Tyr-50 on the Heavy Chain and of Tyr-32 on the Light Chain in the Steroid Combining Site of a Mouse Monoclonal Anti-Estradiol Antibody Using C3-, C6-, and C7-Linked 5-Azido-2-nitrobenzoylamidoestradiol Photoreagents†

Marc Rolland de Ravel,‡ Thierry Blachère,‡ Frédéric Delolme,§ Guy Dessalces,§ Stéphane Coulon,|| Daniel Baty,|| Catherine Grenot,‡ Elisabeth Mappus,‡ and Claude Y. Cuilleron*,‡

Institut National de la Santé et de la Recherche Médicale, Unité INSERM U 329, Pathologie Hormonale Moléculaire, Hôpital Debrousse, 69322 Lyon, France, Service Central d'Analyse, SCA-CNRS-USR59, 69390 Vernaison, France, and Institut de Biologie Structurale et de Microbiologie, Laboratoire d'Ingénierie des Systèmes Macromoléculaires, UPR 9027, CNRS, 31 chemin Joseph Aiguier, 13402 Marseille, France

Received June 7, 2001; Revised Manuscript Received September 17, 2001

ABSTRACT: A mouse monoclonal anti-7-(*O*-carboxymethyl)oximinoestradiol antibody 9D3, raised against the same immunogen as that employed for generating the reported anti-estradiol antibody 15H11 [Rousselot, P., et al. (1997) *Biochemistry 36*, 7860−7868], was found to exhibit an opposite specificity profile with a much stronger recognition of the D-ring than of the A-ring extremity of the steroid, but a similar lack of specificity for both 6- and 7-positions of the B-ring. This antibody was photoaffinity-labeled with five (5-azido-2-nitrobenzoyl)amido (ANBA) derivatives of [17α-^{3}H]estradiol, synthesized from 3-aminoethyloxy, 3-(aminoethylamido)carboxymethyloxy, 6α- and 6*β*-amino, and 7-[*O*-(aminoethylamido)carboxymethyl]oximino precursors. After tryptic digestion, the radioactive peptides on L and H chains were immunopurified with the immobilized antibody 9D3, separated by reversed-phase liquid chromatography, sequenced, and characterized by mass spectrometry, including post-source decay-matrix-assisted laser desorption/ionization time-of-flight mass spectrometry. The long 3-(ANBA-ethylamido)carboxymethyl ether photoreagent was found to label TyrL-32 (on CDR L1), whereas no labeling was observed with the shorter 3-derivative, a result in agreement with a binding pocket large enough to explain the high cross-reactivity with estradiol 3-conjugates. The two 6α- and 6*β*-ANBA-estradiol isomers, as well as the 7-[*O*-(ANBA-ethylamido)carboxymethyl]oximinoestradiol photoreagent derived from the steroid hapten, labeled the same TyrL-32 residue. The 6*β*-ANBA epimer also labeled TyrH-50 (at the basis of CDR H2). These experiments indicate that TyrL-32 is freely accessible from the three C3, C6, and C7 positions, all presumed to be exposed to solvent, while TyrH-50 is probably located on the *β*-face of estradiol. These results, obtained in solution, provide experimental data useful for molecular modeling of the steroid-antibody complex.

Anti-estradiol antibodies with very high affinity and specificity are essential tools for the reliable measurement of plasma estradiol levels by direct and automated immunoassays. To date, conventional hybridoma technology has remained unable to provide anti-estradiol monoclonal antibodies with fully adequate binding properties (*1*, *2*), especially for immunoassays of very low concentrations of estradiol, despite numerous attempts based on structural modifications of hapten structure as well as on the variability of animal immune response.

The specificity of anti-steroid polyclonal or monoclonal antibodies is known to be usually much higher for the region of the steroid opposite or distal to the intermediate arm linking the steroid hapten to the immunogenic carrier protein than for the region in the vicinity of the coupling site. Indeed, the use of estradiol immunogens linked through one of the characteristic functional groups, such as the hydroxyl groups at C3 or C17 positions, led to high cross-reactions either with estradiol 3-sulfate and 3-glucuronide conjugates or with estrone and estriol (*3*−*7*). On the other hand, the introduction of appropriate hapten arms at an intermediate position, i.e., the C6, C7, or C11 positions of estradiol, proved successful to generate polyclonal antibodies specific for both A- and D-rings (*3*, *8*, *9*) but failed to provide a similar specificity profile in the case of monoclonal antibodies. For instance, the use of a 6-(*O*-carboxymethyl)oxime link led to monoclonal antibodies with a high specificity for the A-ring but also with a high cross-reaction with estriol (*4*) as well as to a high specificity for the D-ring but with either unspecified

† This work was supported by the Institut National de la Santé et de la Recherche Médicale (INSERM) and by a grant from Ministère de l'Education Nationale, de l'Enseignement Supérieur et de la Recherche (MENESR−France) "Actions Concertées Coordonnées des Sciences du Vivant" (ACC SV no. 9505207).

* To whom correspondence should be addressed. Phone: (33) 4 78 25 18 08. Fax: (33) 4 78 25 61 68. E-mail: cuilleron@lyon151.inserm.fr.

‡ Institut National de la Santé et de la Recherche Médicale.

§ Service Central d'Analyse.

|| Institut de Biologie Structurale et de Microbiologie.

10.1021/bi011174b CCC: $20.00
Published on Web 11/15/2001

cross-reactions with 3-conjugates (*6*, *10*, *11*) or a high cross-reaction with a 3-sulfate in the case of a closely related anti-6-(*O*-carboxymethyl)oximino-17α-ethynylestradiol monoclonal antibody (*12*). Very recently, two anti-estradiol monoclonal antibodies raised against a 6-ethylmethoxycarbonyl derivative of unspecified stereochemistry have been reported to exhibit also a high specificity for the D-ring but not for the A-ring (*13*). Taken together, these results suggest that the use of estrogenic haptens linked at an intermediate position, such as the C6 position, may not exhibit a much better capacity to induce fully specific anti-estradiol monoclonal antibodies than C3- or C17-linked haptens, owing presumably to a preferred recognition by an isolated monoclonal antibody of only one of the two available A- and D-ring extremities. Moreover, steroid haptens generate a more or less strong immunological recognition of the linker arm, according to its chemical structure, its position on the steroid, and the degree of maturation of antibody response (*14*).

In this laboratory, two monoclonal anti-estradiol antibodies have been generated from the same steroid hapten using an unsaturated exocyclic 7-CMO-link not conjugated with the aromatic ring (in contrast to the more usual 6-CMO-derivatives which may modify phenol recognition) and equidistant from both C3 and C17 positions. The 7-CMO is a rigid group which has been previously shown to exist in a single syn configuration toward C6 position (*15*), confirmed more recently for 7-CMO-estradiol[1] by NMR studies (Mappus, E., et al., unpublished results). One of these antibodies, 15H11, with a high affinity for estradiol (2.4×10^{10} M^{-1}), was found highly specific for the A-ring but was only moderately specific for the D-ring (*16*) whereas the other one, 9D3, reported in this study, also with a high affinity for estradiol (1.3×10^{10} M^{-1}), is highly specific for the D-ring but not for the A-ring. These two antibodies exhibit a lack of specificity for both positions C6 and C7 of the B-ring but remain sensitive to differences in the structures of 6- and 7-substituted estradiol competitors, thus raising the question whether a more or less proximal part of the binding site still embraces this part of the steroid molecule expected to be the most exposed to solvent. On the other hand, the relatively high cross-reactions of antibody 9D3 with estradiol 3-sulfate (51%) and 3-glucuronide (28%) suggest that the C3 position is loosely recognized and possibly partially exposed to solvent.

Recent progress in antibody engineering methodologies has stimulated new promising approaches aimed at modifying the binding properties of anti-steroid antibodies, as illustrated by several reports on anti-testosterone mAbs (*17*), anti-digoxin mAbs (*18*, *19*), anti-cortisol mAbs (*20*), and anti-estradiol mAbs (*1*, *2*, *13*, *21*).

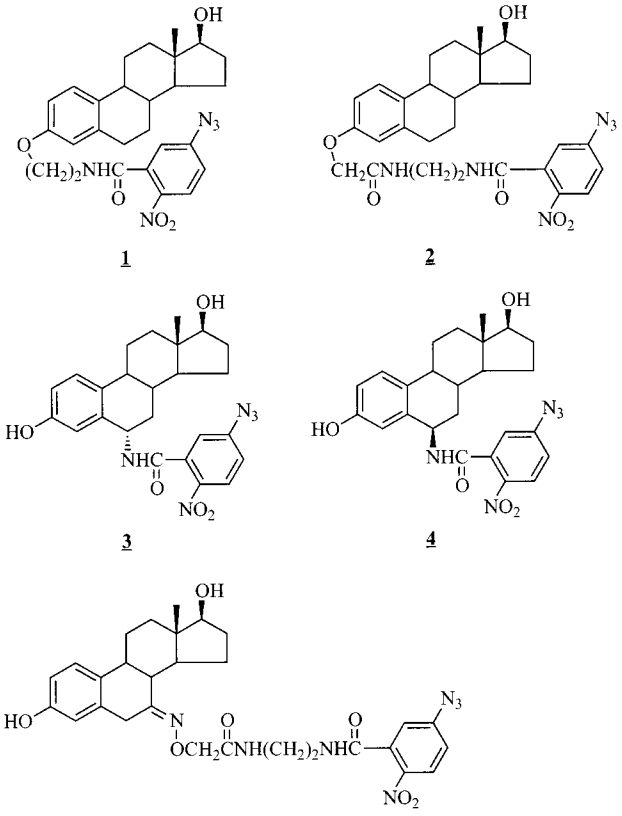

FIGURE 1: Structures of ANBA-estradiol photoaffinity-labeling reagents: 3-ANBA-ethyloxyestradiol (**1**), 3-ANBA-EA-carboxymethylestradiol (**2**), 6α-ANBA-estradiol (**3**), 6*β*-ANBA-estradiol (**4**), and 7-ANBA-EA-CMO-estradiol (**5**).

To support a reasoned approach to improve the specificity of the binding site by genetic engineering, preliminary structural information is needed on anti-estradiol antibody combining sites as well as on the stereochemistry of insertion of steroid derivatives which is particularly important for the selection of the most adequate structures for library panning as well as for the access to modified steroid tracers of appropriate specificity required for immunoassays. Although molecular modeling has become a very powerful tool to provide structural information directly from the amino acid sequences of hypervariable regions of both H and L chains, experimental evidence is still required to confirm proposed models, especially for the two regions of lower specificity corresponding, respectively, to the hapten link and to the less well recognized of the two A- or D-rings, which are the main targets for the design of mutagenesis experiments aimed at improving specificity. In a previous report, affinity-labeling experiments performed on the monoclonal anti-7-CMO-estradiol antibody 15H11, more specific for the A-ring, have revealed that the TyrL-49 residue was the common target of the two epimeric 6α-and 6*β*-ANBA-estradiol photoreagents (*16*). In the present study, photoaffinity-labeling experiments with ANBA-estradiol photoreagents substituted at C3, C6α, C6*β*, and C7 positions of estradiol (Figure 1) were undertaken on the D-ring specific monoclonal anti-7-CMO-estradiol antibody 9D3, to localize the two unspecific

[1] Abbreviations: 3-ANBA-ethyloxyestradiol, estradiol 3-*O*-[2′-(5-azido-2-nitrobenzoyl)amido]ethyl ether; 3-ANBA-carboxymethyloxy-estradiol, estradiol 3-*O*-[2′-(5-azido-2-nitrobenzoyl)amidoethylamido]-carboxymethyl ether; 6α/*β*-ANBA-estradiol, 6α/*β*-(5-azido-2-nitrobenzoyl)amidoestradiol; 7-ANBA-EA-CMO-estradiol, 7-[*O*-(5-azido-2-nitrobenzoyl)amidoethylamidocarboxymethyl]oximinoestradiol; BSA, bovine serum albumin; CDR, complementary determining region; 6- or 7-CMO-estradiol, 6- or 7-(*O*-carboxymethyl)oximinoestra-1,3,5(10)-triene-3,17*β*-diol; DCC, dextran-coated charcoal; DHAS, dehydroepiandrosterone sulfate; DHT, 5α-dihydrotestosterone; H chain, heavy chain; HPLC, high-performance liquid chromatography; L chain, light chain; LSIMS, liquid secondary ion mass spectrometry; mAb, monoclonal antibody; MALDI-TOF-MS, matrix-assisted laser desorption/ionization time-of-flight mass spectrometry; PCR, polymerase chain reaction; PSD, post-source decay; PTH, phenylthiohydantoin; S. A., specific activity; SDS−PAGE, sodium dodecyl sulfate−polyacrylamide gel electrophoresis; TFA, trifluoroacetic acid; TLC, thin-layer chromatography.

regions encompassing the A-ring and the hapten link, respectively, and to define more precisely the orientation of the modified steroid derivatives in the antibody combining site.

EXPERIMENTAL PROCEDURES

Chemicals and Buffers. [2,4,6,7,16,17-$^3H_6$]Estradiol (159 Ci/mmol) and [^{3}H]$NaBH_4$ (11.2 or 13.8 Ci/mmol) were purchased from Amersham. *N*-(5-Azido-2-nitrobenzoyloxy)-succinimide (ANB-NOS reagent) was purchased from Sigma. Other chemical reagents were purchased from Aldrich. *N*-Tosyl-L-phenylalanine chloromethyl ketone-trypsin (TPCK-trypsin) and *N*-tosyl-L-lysine chloromethyl ketone-chymotrypsin (TLCK-chymotrypsin) were from Sigma. The following were also used: phosphate-gelatin (0.1 M phosphate buffer pH 7.4, 0.9% NaCl, 0.1% gelatin, 0.1% sodium azide), Tris-HCl (0.1 M Tris(hydroxymethyl)aminomethane hydrochloride, pH 8.0), Tris-gelatin (0.1 M Tris-HCl, 0.1% gelatin at pH 8.0), Tris-urea (0.1 M Tris-HCl and 6 M urea, pH 8.0), and DCC (5 g of Norit A, 0.5 g of dextran T-70 in 1 L of Tris-HCl at pH 8.0 or of 0.1 M phosphate buffer pH 7.4).

*Synthesis of Radioinert 3-ANBA-Ethyloxyestradiol **1** (Figure 1).* A solution of estradiol 3-aminoethyl ether (*22*) (15 mg, 0.048 mmol) in a mixture of tetrahydrofuran (0.5 mL), pyridine (0.5 mL), and $NaHCO_3$ 0.1 M (10 μL) was acylated by progressive addition of a solution of *N*-(5-azido-2-nitrobenzoyloxy)succinimide (16 mg, 0.052 mmol) in tetrahydrofuran (0.5 mL). The reaction mixture was stirred for 24 h at 22 °C in the dark and evaporated under a nitrogen stream. The crude product was purified by TLC on silica gel (toluene/ethyl acetate 1:1, R_f 0.50; chloroform/methanol 10:1, R_f 0.40) to give the 3-ANBA-ethyl ether derivative (14 mg, 0.028 mmol, 58%) as a pale yellow solid. Purity of this derivative was confirmed by HPLC (C_{18} Ultrabase column, Waters; acetonitrile−water 60:40; flow rate = 0.8 mL /min; retention time = 15.0 min).

Melting point (mp) (recrystallized from ethyl acetate) 92−94 °C; λ_{max} (EtOH) at 289 nm (ϵ = 11 000 M^{-1} cm^{-1}) and 308 nm (ϵ = 10 400 M^{-1} cm^{-1}); ^{1}H NMR (C_5D_5N) δ 1.01 (3H, s, 18-CH_3), 3.94 (1H, m, 17α-H), 4.12 (2H, t, J = 5.3 Hz, OCH_2), 4.38 (2H, t, J = 5.3 Hz, CH_2N), 6.78 (1H, d, J = 2.6 Hz, H-4), 6.91 (1H, dd, J = 8.8 and 2.6 Hz, H-2), 7.11 (1H, dd, J = 8.8 Hz, and 2.5 Hz, H-4′), 7.27 (1H, d, J = 8.8 Hz, H-1), 7.52 (1H, d, J = 2.5 Hz, H-6′), 8.05 (1H, d, J = 8.8 Hz, H-3′); high-resolution MS (LSIMS) calculated for $C_{27}H_{32}O_5N_5$ (MH^+), 506.2403; found, 506.2403.

*Synthesis of Radioinert 3-ANBA-EA-Carboxymethyloxyestradiol **2** (Figure 1).* The *N*-hydroxysuccinimide ester derivative of estradiol 3-*O*-carboxymethyl ether (*23*, *24*) (100 mg, 0.23 mmol) was dissolved in tetrahydrofuran (1.5 mL) containing $NaHCO_3$ 0.1 M (100 μL) and stirred overnight with an excess of ethylenediamine (80 μL, 1.02 mmol). After evaporation of the solvent, the crude residue was purified by TLC on silica gel (chloroform/methanol/NH_4OH 100:20:5, R_f 0.47) to give the amine (16 mg, 0.043 mmol) which was acylated with *N*-(5-azido-2-nitrobenzoyloxy)succinimide, as described above. The crude product was purified by TLC on silica gel (chloroform/methanol 10:1, R_f 0.38) to give the 3-ANBA-EA-carboxymethyl ether derivative (14 mg, 0.025 mmol, 59%) as a white solid. Purity of this derivative was confirmed by HPLC (C_{18} Ultrabase column, Waters; acetonitrile-water 60:40; flow rate = 0.8 mL /min; retention time = 8.6 min).

Mp (recrystallized from ethyl acetate) 170−171 °C; λ_{max} (EtOH) at 289 nm (ϵ = 11 000 M^{-1} cm^{-1}) and 308 nm (ϵ = 9700 M^{-1} cm^{-1}); ^{1}H NMR (C_5D_5N) δ 0.99 (3H, s, 18-CH_3), 3.93 (5H, s broad, $N(CH_2)_2N$ and 17α-H), 4.79 (2H, s, OCH_2), 6.76 (1H, d, J = 2.6 Hz, H-4), 6.90 (1H, dd, J = 8.6 and 2.6 Hz, H-2), 7.10 (1H, dd, J = 8.8 and 2.5 Hz, H-4′), 7.24 (1H, d, J = 8.6 Hz, H-1), 7.59 (1H, d, J = 2.5 Hz, H-6′), 8.06 (1H, d, J = 8.8 Hz, H-3′); high-resolution MS (LSIMS) calculated for $C_{29}H_{35}O_6N_6$ (MH^+), 563.2618; found, 563.2621.

*Synthesis of Radioinert 6α- and 6β-ANBA-Estradiol **3** and **4** (Figure 1).* These two derivatives were prepared as previously described (*2*).

*Synthesis of Radioinert 7-ANBA-EA-CMO-Estradiol **5** (Figure 1).* 7-CMO-Estradiol (*25*) (31 mg, 0.087 mmol) was converted to an *N*-hydroxysuccinimide ester and condensed with ethylenediamine, as described above. The product was purified by TLC on silica gel (chloroform/methanol/NH_4-OH 100:40:9, R_f 0.50) to give the amine (10 mg, 0.025 mmol) which was acylated with *N*-(5-azido-2-nitrobenzoyloxy)succinimide. The crude product was purified by TLC on silica gel (chloroform/methanol 10:1, R_f 0.26) to give the 7-ANBA-EA-CMO derivative (12 mg, 0.020 mmol, 82%) as a white solid. Purity of this derivative was confirmed by HPLC (C_{18} Ultrabase column, Waters; acetonitrile-water 70:30; flow rate = 0.8 mL/min; retention time = 6.1 min).

Mp (recrystallized from ethyl acetate) 115−117 °C; $[\alpha]_D$ = +30° (EtOH); λ_{max} (EtOH) at 289 nm (ϵ = 10 100 M^{-1} cm^{-1}) and 309 nm (ϵ = 10 800 M^{-1} cm^{-1}); ^{1}H NMR (C_5D_5N) δ 0.97 (3H, s, 18-CH_3), 3.92 [5H, m broad, $N(CH_2)_2N$ and 17α-H], 4.94 (2H, s, OCH_2), 6.92 (1H, d, $J \sim 3$ Hz, H-4), 7.09 (4H, 2 dd superimposed, H-2 and H-4′), 7.25 (1H, d, J = 8.2 Hz, H-1), 7.56 (1H, d, J = 2.5 Hz, H-6′), 8.00 (1H, d, J = 8.8 Hz, H-3′); high-resolution MS (LSIMS) calculated for $C_{29}H_{34}O_7N_7$ (MH^+), 592.2520; found, 592.2520.

Synthesis of Radioactive [17α-^{3}H]Estradiol Analogues of 3-ANBA-Ethyloxyestradiol, 3-ANBA-EA-Carboxymethyloxyestradiol, and 7-ANBA-EA-CMO-Estradiol Photoaffinity-Labeling Reagents. Each of the three radioinert ANBA-estradiol precursors (0.015 mmol) was dissolved in acetone (50 mL) at 4 °C and oxidized by Jones reagent (*26*) (40 μL). The reaction was stirred for 30 min at 4 °C. The reaction was stopped by addition of NH_4OH 25% (40 μL). After evaporation of the solvent, the product was purified by TLC on silica gel (chloroform/methanol 10:1 v/v). The purified estrone intermediate was dissolved in ethanol (200 μL) and reduced by stirring for 15 min at 4 °C with a solution of [^{3}H]$NaBH_4$ (10 mCi) in methanol (20 μL). After evaporation under a stream of nitrogen, the product was purified immediately by TLC on silica gel plates (5 × 7.5 cm, Macherey-Nagel, chloroform/methanol 10:1 v/v), in the dark, under nitrogen or argon atmosphere. The purified reduced compound was controlled by HPLC coupled with an on-line radioactivity detector (Flo-one, Packard Instruments). The TLC R_f values and the HPLC retention times of all radioactive compounds were superimposable to those of the corresponding radioinert ANBA-estradiol derivative.

Production, Purification, and Characterization of the Monoclonal Antibody 9D3. Production and purification of the monoclonal anti-estradiol antibody 9D3, size-exclusion HPLC, chromatofocusing, gel electrophoresis, determination of antibody binding characteristics, and cDNA sequencing of L and H chains were performed as reported for the anti-estradiol antibody 15H11 (*16*), except for binding measurements which were made in a phosphate-gelatin buffer.

Photoaffinity-Labeling. The ascitic fluid containing the antibody 9D3 (4 mL, 72 nmol, i.e., 144 nmol of steroid binding sites was incubated with an equimolecular amount (144 nmol) of the following photoreagents containing the corresponding [17α-^{3}H]estradiol analogue as tritiated tracer: 3-ANBA-ethyloxyestradiol or 3-ANBA-EA-carboxymethyloxyestradiol (including $\sim 11 \times 10^6$ dpm, 1.4 nmol and 110×10^6 dpm, 14.4 nmol of tritiated tracer of S. A. = 3.45 Ci/mmol, respectively), 6α- and/or 6β-ANBA-estradiol (including $\sim 20 \times 10^6$ dpm, 3.2 nmol of tritiated tracer of S. A. = 2.8 Ci/mmol, in both cases), or 7-CMO-AE-ANBA-estradiol derivative (including $\sim 50 \times 10^6$ dpm, 8.0, or 6.5 nmol of tritiated tracer of S. A. = 2.8 or 3.45 Ci/mmol, respectively), in 8 mL of Tris-HCl, pH 8.0 buffer, overnight at 4 °C, in the dark, under argon atmosphere. The irradiation step was realized as previously described (*16*). Some experiments for mass spectrometry analysis were performed in the absence of radioactive tracer.

Preparation, Enzymatic Cleavage, and Purification of Photoaffinity-Labeled Peptides. Purification of the photoaffinity-labeled antibody on immobilized Protein G, separation and enzymatic cleavage of labeled H and L chains, and immunopurification of the photolabeled tryptic peptides were realized according to protocols previously reported for antibody 15H11 (*16*). Chymotryptic subcleavage of the crude tryptic digest was performed with TLCK-chymotrypsin.

HPLC purification of photoaffinity-labeled tryptic peptides was performed on a C_{18} column (Macherey-Nagel Nucleosil, 100 Å, 0.46 × 15 cm) using an aqueous acetonitrile gradient (0−5 min with 0% acetonitrile, 5−10 min with 0 to 25% acetonitrile, 10−50 min with 25 to 45% acetonitrile, and 50−55 min with 100% acetonitrile) in the presence of 0.1% TFA, at a flow-rate of 1 mL/min. Peptide profiles were monitored by UV at 220, 280, and 410 nm and by radioactivity, determined on-line with a Flo-one Packard radiodetector. For photolabeling experiments performed with radioinert 3-ANBA-EA-carboxymethyloxyestradiol and 7-ANBA-EA-CMO-estradiol photoreagents, the HPLC profiles were monitored by UV absorption at 410 nm (*16*), which provided an efficient alternative to radioactivity, that led to the same (superimposable) peaks.

Edman Sequence Determinations. Edman sequence determinations were performed in a gas-phase sequencer equipped with an on-line phenylthiohydantoin (PTH) analyzer (Applied Biosystems, model 470 sequencer). Photolabeled peptides were sequenced directly while N-terminal sequences of separated H and L antibody chains were determined on samples electroblotted on Immobilon-P membranes.

Mass Spectrometry. Liquid secondary ion mass spectra (Cs^+) were recorded either with a VG ZAB 2SEQ or a Finnigan-MAT 95XL mass spectrometer using a thioglycerol-1% TFA matrix. Electrospray mass spectra were recorded with a Hewlett-Packard 5989 mass spectrometer. For the electrospray ion source, the capillary exit voltage was 300 V, the resolution was 1000 (50% valley), and the quadrupole was scanning from *m*/*z* 250 to 2000. A liquid chromatography-electrospray ionization mass spectrometer setup was also employed (Waters Micromass) combining an HPLC apparatus (Waters 2690-Alliance, C_{18} Symmetry column, water-acetonitrile-0.1% TFA gradient) and a ZMD 4000 mass spectrometer (positive electrospray source, scanning range = 800−2400). MALDI-TOF mass spectra were recorded on a Voyager-DE STR mass spectrometer (nitrogen laser at 337 nm) in the linear or reflector mode as well as in the PSD mode, using an α-cyano-4-hydroxycinnamic acid matrix, a positive polarity, an accelerating voltage of 20 or 25 kV, an extraction delay time varying from 75 to 150 ns, and an appropriate acquisition mass range ($M < 3000$) or fragment ion window (PSD). The peptide (1−4 pmol, solubilized in acetonitrile after desalting) was spotted and dried on the sample supporting device. The *m*/*z* values are expressed in Thomson (Th) units and are estimated to be accurate to ±1 in the PSD mode. Calculated masses are expressed in daltons (Da).

RESULTS

Production, Purification, and Characterization of the Monoclonal Anti-Estradiol Antibody 9D3. The mouse monoclonal anti-7-CMO-estradiol antibody 9D3 was characterized as an IgG_1 of the κ class and was therefore purified from mouse ascites fluid by chromatography on immobilized Protein G. The purified immunoglobulin was controlled by SDS−PAGE and by size-exclusion HPLC, which showed a single peak (representing more than 95% of the total absorbance at 280 nm in HPLC). Chromatofocusing revealed a single peak (isoelectric point of 5.52). Completely reduced and alkylated H and L chains were separated by size-exclusion HPLC as two distinct peaks (UV detection at 280 nm) with retention times of 19 and 24 min, respectively. The separated H and L chains were characterized by Edman sequencing of 15 N-terminal amino acid residues (EVQLQQSGPELVKPG) and (DIQMTQSPASLSASV), respectively.

cDNA Sequence Determination. The nucleotide sequences for H and L chain variable regions (Figure 2) were determined using anchored PCR as previously reported for the anti-7-CMO-estradiol antibody 15H11 (*16*). The $V_H/D/J_H$ region of the γ_1 H chain used the IgHV14S12 family and IgHD-ST4 or IgHD-SP2 and IgHJ3.01 gene segments while the V_K/J_K region of L chain was found to correspond to the IgKV12−41.01 family and IgKJ1.01 gene segment, as determined by comparison with mouse IgG nucleotidic sequences of the Immunogenetics (IGMT) database (http://imgt.cines.fr.81104). The amino acid sequence of the variable region of H chain was found most homologous (77%) with an anti-DNA antibody (*27*) and also with three other anti-DNA antibodies (*28*). The amino acid sequence of the variable region of L chain was found to have a very high homology (88%) with anti-estradiol antibody 57-2 (*29*) as well as with anti-DNA antibodies (*28*) and an anti-horse cytochrome *c* antibody (*30*, *31*). The amino acid sequences of the variable regions of H and L chains of antibody 9D3 were aligned with those reported for two other anti-estradiol antibodies 57-2 (*29*) and 15H11 (*16*) (Figure 3). The amino acid sequence numbering and the identification of hypervariable regions (CDRs) were made according to conven-

9D3 L chain variable region sequence:

1 FR																			
gac	atc	cag	atg	act	cag	tct	cca	gcc	tcc	cta	tct	gca	tct	gtg	gga	gaa	act	gtc	acc
D	I	Q	M	T	Q	S	P	A	S	L	S	A	S	V	G	E	T	V	T
21			CDR1											FR2					
atc	aca	tgt	cga	gca	agt	ggg	aat	att	cac	aat	tat	tta	gca	tgg	tat	cag	cag	aaa	cag
I	T	C	**R**	**A**	**S**	**G**	**N**	**I**	**H**	**N**	**Y**	**L**	**A**	W	Y	Q	Q	K	Q
41									CDR2							FR3			
gga	aaa	tct	cct	cag	ctc	ctg	gtc	tat	aat	gca	aac	acc	tta	gcg	gga	ggt	gtg	cca	tca
G	K	S	P	Q	L	L	V	Y	**N**	**A**	**N**	**T**	**L**	**A**	**G**	G	V	P	S
61																			
aga	ttc	agt	ggc	agt	gga	tca	gga	aca	caa	ttt	tct	ctc	acg	atc	aac	agc	ctg	cag	cct
R	F	S	G	S	G	S	G	T	Q	F	S	L	T	I	N	S	L	Q	P
81								CDR3									FR4		
gaa	gat	ttt	ggg	aat	tat	tac	tgt	cat	ctt	tat	tct	agt	att	ccg	tgg	tcg	ttc	ggt	gga
E	D	F	G	N	Y	Y	C	**H**	**L**	**Y**	**S**	**S**	**I**	**P**	**W**	**S**	F	G	G
101						107													
ggc	acc	aga	ctg	gaa	atc	aag													
G	T	R	L	E	I	K													

9D3 H chain variable region sequence:

1 FR																			
gag	gtc	cag	ctg	cag	cag	tct	gga	cct	gaa	ctg	gta	aag	cct	ggg	gct	tca	gta	aag	atg
E	V	Q	L	Q	Q	S	G	P	E	L	V	K	P	G	A	S	V	K	M
21										CDR1					FR2				
tcc	tgc	aag	gct	tct	gga	tac	aca	ttc	act	aga	ttt	att	tcg	caa	tgg	gtg	aag	cag	agg
S	C	K	A	S	G	Y	T	F	T	**R**	**F**	**I**	**S**	**Q**	W	V	K	Q	R
41									CDR2										
cct	ggg	cag	ggc	ctt	gag	tgg	att	gga	tat	ttg	gat	cct	tac	agt	ggc	ggt	cct	aaa	tac
P	G	Q	G	L	E	W	I	G	**Y**	**L**	**D**	**P**	**Y**	**S**	**G**	**G**	**P**	**K**	**Y**
61						FR3													
agt	gag	aag	ttc	aaa	ggc	aag	gcc	act	ctg	act	gca	gac	ata	ttc	tcc	aac	aca	gcc	tac
S	**E**	**K**	**F**	**K**	**G**	K	A	T	L	T	A	D	I	**F**	S	N	T	A	Y
81																		CDR3	
atg	gaa	ctc	agc	agc	ctg	acc	tct	gag	gac	tct	gcg	gtc	tat	ttc	tgt	gga	agg	gta	gac
M	E	L	S	S	L	T	S	E	D	S	A	V	Y	F	C	G	R	**V**	**D**
101				FR4										115					
ggc	tcg	ggc	cac	tgg	ggc	caa	ggg	act	ctg	gtc	act	gtc	tct	gca					
G	**S**	**G**	**H**	W	G	Q	G	T	L	V	T	V	S	A					

FIGURE 2: Nucleotide sequences of L and H chain variable regions (see Experimental Procedures). The CDR regions of each chain are underlined (nucleotides) or in bold characters (amino acids), according to the Kabat system (*32*).

tional nomenclatures of Kabat (*32)* in Figure 1 and of Chothia and Lesk *(33*) in Figure 2.

Antibody Binding Characteristics. The cross-reactions of estradiol competitors with the anti-7-CMO-estradiol antibody 9D3 (Table 1) revealed a high specificity for the 17β-hydroxy group toward estrone, estriol, or 17α-hydroxyestradiol, a lack of specificity for the 3-hydroxy group toward estradiol 3-sulfate and 3-glucuronide conjugates, and a low specificity for 6- and 7-positions of B-ring through which the 7-CMO-estradiol hapten was linked to the immunogenic protein. The two short and long 3-ANBA-ethyloxyestradiol and 3-ANBA-EA-carboxymethyloxyestradiol photoreagents showed higher cross-reactions (93 and 106%, respectively) than estradiol 3-sulfate and 3-glucuronide (51 and 28%, respectively). The cross-reaction measured with the 6α-ANBA-estradiol photoreagent was much higher (103%) than that found with the 6β-ANBA-estradiol epimer (33%), as expected from the relative coplanarity of the equatorial 6α-ANBA isomer with the 7-CMO substituent which should favor insertion in the subsite region corresponding to the 7-CMO hapten link. Moreover, the lower cross-reaction of the axial 6β-epimer probably reflects an increased steric hindrance on the β-side of the steroid. Surprisingly, the cross-reactivity with 7-ANBA-EA-CMO-estradiol photoreagent, structurally derived from the haptenic steroid employed in the immunogen (110%), was lower than that observed for the isomeric 6-ANBA-EA-CMO-estradiol derivative (160%), not employed as photoreagent in this study. Such a difference suggests that the C6 position is more exposed to solvent than the C7 position of the hapten link. A more detailed inspection of the specificity data indicates that, despite the high cross-reactivity with 3-conjugates, the aromatic A-ring is unambiguously differentiated from an enone ring or a saturated 3β-hydroxy-A-ring, as shown by the low cross-reactions of testosterone (0.1%) and 19-nortestosterone (2.8%) or androst-5-ene-3β,17β-diol ($<$0.2%). A low cross-reactivity was also observed with 2-methoxyestradiol (2%) as well as with 2-iodoestradiol (8%) while a much higher cross-reactivity was observed with 4-methoxyestradiol (82%) and even the larger 4-iodoestradiol (20%), thus suggesting that the C2 side of A-ring is more buried than the C4 side, contiguous to the solvent-exposed C3, C6, and C7 positions. The very low cross-reaction with 11α-hydroxyestradiol ($<$0.2%) indicates that the C11 side of C-ring is probably also buried, as presumed for C2 and C17 positions on the same side.

The association constants for 3-ANBA-EA-carboxymethyloxy-[17α-^{3}H]estradiol (1.6×10^{10} M^{-1}), 6α- and 6β-ANBA-[17α-^{3}H]estradiol (1.4×10^{10} and 1.2×10^{10} M^{-1}, respectively), and 7-ANBA-EA-CMO-[17α-^{3}H]estradiol (3.7×10^{10} M^{-1}), estimated from Scatchard plots established by equilibrium dialysis experiments at 4 °C performed directly on ascitic fluid (Figure 4), were found to correspond in magnitude to the association constant measured similarly for estradiol ($\sim 1.3 \times 10^{10}$ M^{-1}), using [2,4,6,7,16,17-^{3}H$_6$]-estradiol. The association constant for the unreactive 3-ANBA-ethyloxyestradiol photoreagent (vide infra) was measured only approximately ($\sim 10^{10}$ M^{-1}, data not shown). These association constants are in agreement with the order of the corresponding cross-reactions. However, the sensitivities of these two binding parameters to the photoreagent structures were significantly different, owing probably to differences in the relative recognition of the estradiol and side-chain parts of these derivatives, as illustrated for the 7-ANBA-EA-CMO-estradiol structure derived from that of the immunogen,

```
L chain variable region sequence
                FR1          |       CDR1       |      FR2       | CDR2  |           FR3                    |      CDR3       |  FR4
     1        10        20              30        40         50       60        70        80         90               100
     .         .         .       abcdef .          .          .         .         .         .          .                .
9D3   DIQMTQSPASLSASVGETVTITC RASG******NIHNYLA WYQQKQGKSPQLLVY NANTLAG GVPSRFSGSGSGTQFSLTINSLQPEDFGNYYC HLYSSIP******WS FGGGTRLEIKR
57-2  DIQMTQSPASLSASVGETVTITC RASG******NIHNYLA WYQQKQGKSPQLLVY NAKTLAD GVPSRFSGSGSGTQYSLKINSLQPEDFGTYYC HHFWSTP******WT FGGGTKLEVKR
15H11 DIVMTQSPASISVSLGDTVSITC HAS******QGINSNIG WLQLKPGKSFKGLMY HGNTLED GIPSRFSGSGSGGIYSLTINSLEFEDFAVYYC VQYAQFP******RT FGGGTRLEIK

H chain variable region sequence
                FR1            | CDR1   |        FR2        | CDR2   |                  FR3                   |       CDR3        |   FR4
     1        10        20        30         40         50      60        70        80         90          100                 110
     .         .         .       . ab         .          .   abc    .         .         .  abc      .         .abcdefghijk          .
9D3   EVQLQQSGPELVKPGASVKMSCKAS GYTFTR**F ISQWVKQRPGQGLEWIGYL DP**YSGG PKYSEKFKGKATLTADIFSNTAYMELSSLTSEDSAVYFCGR VDGS*************GH WGQGTLVTVSA
57-2  QIQLVQSGPELKKPGETVRISCKAS DYSFMT**S GMQWVQQMPGKGLKWIGWL NT**QSGV PEYAEDFKGRFAFSLETSATTAYLQINNLKNEDTATYFCAT WGGNS************AY WGQGTTLTVSS
15H11 QVLLQQPITELARPGTSVKLSCKAS GYAFPS**H VMSWVKQISGQGLEWIGEI YP**RSGN SYYNENFKDRATLTADRSSNTVYMEVSSLTTEDSAVYFCGF G****************KE WGQGTTLTVSS
```

FIGURE 3: Amino acid sequence alignments of L and H chain variable regions of monoclonal anti-estradiol antibodies 9D3, 57-2, and 15H11). The hypervariable regions are aligned according to Chothia and Lesk (*33*).

Table 1: Binding Specificity of Monoclonal Anti-Estradiol Antibody 9D3 for Steroid Analogues

steroids	% cross-reaction[a]
estradiol	100
D-ring modifications	
estrone	0.03
estriol (16α-hydroxyestradiol)	0.3
17α-estradiol	<0.2
A-ring modifications	
2-methoxy	2
2-iodo	8
3-sulfate	51
3-glucuronide	28
3-ANBA-ethyl ether	93
3-ANBA-ethylamidocarboxymethyl ether	106
4-methoxy	82
4-iodo	20
B-ring modifications	
6-oxo	36
6-ANBA-EA-CMO	160
6α-ANBA	103
6β-ANBA	33
6α-bromoacetamido	20
6β-bromoacetamido	15
7-oxo	5
7-CMO	11
7-ANBA-EA-CMO	110
7-CMO-histamine	28
7α-hemiglutaramide histamine	4
7β-hemiglutaramide histamine	0.03
7α-hemiglutarate-histamine	13
Δ^6-estradiol	14
C-ring modification	
11α-hydroxy	<0.2
$\Delta^{9(11)}$-estradiol	12.5
other steroids	
testosterone	0.1
DHT	0.2
19-nortestosterone	2.8
androst-4-ene-3β,17β-diol	<0.2
DHAS	0.64
progesterone	<0.001
21-deoxycortisol	13
cortisol	<0.001
estrone 3-sulfate	<0.002

[a] The percent cross-reactions were determined as the ratio of the moles of radioinert estradiol (× 100) to the moles of competing steroids required to displace 50% of the [^{3}H]estradiol tracer.

which showed an affinity well-above that of estradiol but only a slightly higher cross-reaction, while a much lower cross-reaction was observed for 6β-ANBA-estradiol although the affinity remained only slightly lower than that of estradiol.

Time Course of Photolysis of the Photoaffinity-Labeling Reagents. Photolysis of 3-ANBA-ethyloxyestradiol, 3-ANBA-EA-carboxymethyloxyestradiol, 6α- and 6β-ANBA-estradiol, and 7-ANBA-EA-CMO-estradiol photoreagents in a Tris-HCl, pH 8.0, buffer-ethanol 97:3 mixture, at $\lambda > 300$ nm, using a 2 mm-thick Pyrex filter (*34*) was performed at 4 °C under an argon atmosphere and was almost complete by about 10−15 s while much smaller modifications of UV absorption spectra persisted up to 30−45 min. The UV absorption profiles of all these photolyzed ANBA photoreagents (data not shown) were essentially identical to those previously determined at similar irradiation times for the 6α- and 6β-ANBA-estradiol epimers (*16*).

Photolabeling of Antibody 9D3 with 3-ANBA-Ethyloxyestradiol, 3-ANBA-EA-Carboxymethyloxyestradiol, 6α- and

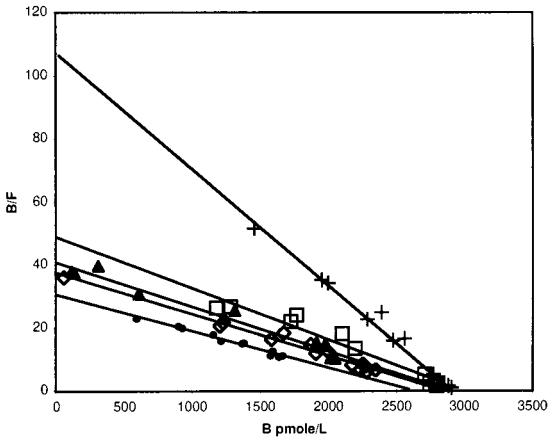

FIGURE 4: Scatchard plots for the binding of estradiol (◊), 3-ANBA-EA-carboxymethylestradiol (□), 6α-ANBA-estradiol (▲), 6β-ANBA-estradiol (●), and 7-ANBA-EA-CMO-estradiol (+) photoreagents with monoclonal anti-estradiol antibody 9D3 in ascitic fluid. The antibody solution, at the dilution 1/60000, in phosphate-gelatin buffer at pH 7.4, was dialyzed for 48 h at 4 °C against increasing amounts of tritiated estradiol or photoreagents (0.2−10-fold molar excess per steroid binding site) placed outside the dialysis bag, in 10 mL of the same buffer.

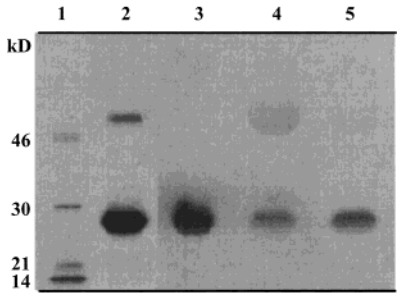

FIGURE 5: SDS−PAGE (10% acrylamide) analysis of unseparated H and L chains of completely reduced and alkylated anti-estradiol antibody 9D3 photolabeled with C3-, C6-, or C7-linked derivatives of [17α-^{3}H]estradiol, revealed by fluorography: ^{14}C molecular mass markers (Amersham), lysozyme, trypsin inhibitor, carbonic anhydrase, and ovalbumin (lane 1), antibody 9D3 photolabeled with 3-ANBA-EA-carboxymethyl-[17α-^{3}H]estradiol (36 μM, 69 560 dpm) (lane 2), antibody 9D3 photolabeled with 6α-ANBA-[17α-^{3}H]estradiol (180 μM, 319 260 dpm) (lane 3), antibody 9D3 photolabeled with 6β-ANBA-[17α-^{3}H]estradiol (180 μM, 127 260 dpm) (lane 4), antibody 9D3 photolabeled with 7-ANBA-EA-CMO-[17α-^{3}H]estradiol (180 μM, 111 216 dpm) (lane 5).

6β-ANBA[17α-^{3}H]Estradiol, and 7-ANBA-EA-CMO-Estradiol Photoaffinity Reagents. The ascitic fluid containing antibody 9D3 (rather than the purified antibody, often found to give aggregates after purification and storage) was incubated with a stoichiometric amount of photoreagent (2 mol/mol antibody) and irradiated at $\lambda > 300$ nm, for 30 min at 4 °C (*35*, *36*). The crude photoreaction mixture was purified on Protein G-agarose, completely reduced and alkylated, and analyzed by SDS−PAGE. Covalent labeling was observed for all tested photoreagents except for the short 3-ANBA-ethyloxyestradiol derivative. As shown by autoradiograms (Figure 5), in all cases, the major fraction of covalently bound radioactivity was localized on the L chain, either exclusively for the 6α-ANBA-estradiol or almost totally for 3-ANBA-EA-carboxymethyloxyestradiol and 7-ANBA-EA-CMO-estradiol photoreagents. The 6β-ANBA-estradiol photoreagent was also recovered predominantly on the L chain, but a significant fraction was found on the H chain (70 and 30% of total labeling on L and H chain, respectively). Control experiments of irradiation of the antibody without photoreagent showed that the antibody-binding properties for estradiol were not altered in the conditions employed for photoaffinity-labeling studies.

Enzymatic Cleavage of Photoaffinity-Labeled Antibody H or L Chains and Purification of Photoaffinity-Labeled Peptides. Tryptic cleavage was performed after complete reduction and alkylation, either directly on the unseparated mixture of H and L chains (6α-ANBA-estradiol and 7-ANBA-EA-CMO-estradiol) or after separation of photoaffinity-labeled H or L chains (3-ANBA-EA-carboxymethyloxy-estradiol and 6β-ANBA-estradiol). After photolabeling with 3-ANBA-EA-carboxymethyloxyestradiol, the crude tryptic digest was also subcleaved by chymotrypsin in order to obtain shorter labeled fragments for analyses by mass spectrometry.

The photolabeled peptides were immunopurified (*37*) with the anti-estradiol antibody 9D3 immobilized on Sepharose 4B. A large excess of immobilized antibody was used in order to obtain a maximum of retention of photolabeled peptides. Elution of the retained peptide fraction was performed with a water-dioxane 7:3 (v/v) mixture (*16*). After this immunopurification step, the maximal percentage of recovery of the total radioactivity added in equimolecular amount for photoaffinity-labeling was 20% for the 3-ANBA-EA-carboxymethyl ether derivative, 14% for the 6α-ANBA derivative, 20% for the 6β-ANBA derivative, and 28% for the 7-ANBA-EA-CMO derivative. These values correspond approximately to the maximal yields of covalent labeling, since only traces of unbound photolyzed photoreagent were detected by HPLC, owing to prior elimination by ultrafiltration after the reduction-alkylation step and to strong absorption on Sepharose during the immunopurification step.

The HPLC radioactivity profiles of the tryptic digests showed several peaks. Studies were limited either to a single major peak, for photolabeling experiments with 3-ANBA-EA-carboxymethyloxy-[17α-^{3}H]estradiol (retention time = 41 min, 32% of eluted radioactivity), 6β-ANBA-[17α-^{3}H]-estradiol (L chain peptide, retention time = 27 min, 13% of eluted radioactivity; H chain peptide, retention time = 41 min, 19% of eluted radioactivity), and 7-ANBA-EA-CMO-[17α-^{3}H]estradiol (retention time = 31 min, 12% of eluted radioactivity), or to the two main peaks, for photolabeling experiments with 6α-ANBA-[17α-^{3}H]estradiol (retention times = 33 and 34 min, 14 and 16% of eluted radioactivity, respectively). In some experiments with 7-ANBA-EA-CMO-[17α-^{3}H]estradiol, another more retained radioactive peak (retention time = 32 min) was observed, which, in one case, was found to reach an intensity similar to the main peak at 31 min, leading to a double peak similar to that mentioned above for 6α-ANBA-[17α-^{3}H]estradiol. The rest of the radioactivity was distributed among 7−12 smaller peaks eluted between 20 and 45 min which were not further studied, except for one peak (retention time = 26 min) which was isolated in one of the photolabeling experiments with 7-ANBA-EA-CMO-[17α-^{3}H]estradiol.

The HPLC profile of the immunopurified mixture of peptides photoaffinity-labeled with radioactive or radioinert 3-ANBA-EA-carboxymethyloxyestradiol, obtained after two successive tryptic and chymotryptic cleavages, revealed two predominant peaks (retention times = 35 and 38 min) not

Table 2: Amino Acid Sequence Analysis of L Chain Peptides Photolabeled with 3-ANBA-EA-Carboxymethylestradiol and 6α-ANBA-Estradiol

		3-ANBA-EA-carboxymethylestradiol-peptide		6α-ANBA-estradiol-peptides			
		peptide 25−35 L (110 288 dpm) 144 pmol[a]		peptide 25−35 L (116 500 dpm) 761 pmol[a]		peptide 25−36 L (137 002 dpm) 895 pmol[a]	
cycle no.	amino acid	PTH derivative (pmol)	radioactivity (dpm)	PTH derivative (pmol)	radioactivity (dpm)[d]	PTH derivative (pmol)	radioactivity (dpm)
1	A	66	979	115	-	138	4322
2	S	36	562	30	-	34	4602
3	G	40	602	54	-	80	3944
4	N	34	856	61	-	80	3220
5	I	37	535	92	-	99	2901
6	H	15	444	35	-	70	2158
7	N	22	1214	44	-	70	2200
8	Y	7.3[b]	5601	nd[c]	-	63[b]	9618
9	L	16	3598	35	-	53	6917
10	A	16	1894	15	-	47	4673
11	W	1	1174	nd[c]	-	nd[c]	3987
12	Y		801			12	3144
13	Q		684				3058
14	Q		510				2492
15	K						2050
16							1692
17							1792
18							1550
filter			28 269				7991

[a] Picomoles of labeled peptide applied to the sequencer calculated from the specific activity of the corresponding radioactive photoreagent. [b] Picomoles of labeled amino acid estimated from the radioactivity eluted at this Edman cycle (no PTH derivative of the unlabeled amino acid was detected at this cycle). [c] Not determined (no corresponding PTH derivative was detected at this cycle). [d] Not measured.

present after tryptic cleavage only and six small peaks. The HPLC purification of tryptic and chymotryptic peptides photolabeled with 3-ANBA-EA-carboxymethyloxyestradiol led to slightly higher retention times than for other photoreagents due to the use of a new column.

Edman Sequencing of Photoaffinity-Labeled Peptides. The major immunopurified tryptic peptide of L chain photolabeled with 3-ANBA-EA-carboxymethyloxy-[17α-^{3}H]-estradiol was identified as the fragment 25−35 A−S−G−N−I−H−N−(X*)−L−A−W (Table 2). The C-terminal chymotryptic subcleavage of this tryptic peptide, observed after TrpL-35, might be due to the use of large amounts of TPCK-trypsin and of prolonged incubation times, both necessary to improve the yield of enzymatic cleavage of antibody chains but also prone to promote side-reactions of enzymatic contaminants either already present in the commercial enzyme (not chosen among the highest sequencing grades), or resulting from a partial degradation (*38*, *39*). In this peptide, no detectable PTH derivative could be found at the 8th Edman cycle corresponding to TyrL-32 which also corresponded to the major peak of eluted radioactivity, indicating that TyrL-32 is the major site of labeling. However, only a very low amount of PTH derivative was observed at the last cycle corresponding to TrpL-35. Therefore, complementary mass spectrometry studies were undertaken on this peptide, as well as on its chymotryptic subfragments 25−32 and 25−33, which confirmed that TyrL-32 is the unique site of photolabeling (vide infra). The presence of the peptide 25−32 also indicates that labeling of TyrL-32 does not prevent chymotryptic cleavage after this residue.

The Edman sequence of the two major radioactive tryptic peptides of the L chain photolabeled with 6α-ANBA-[17α-^{3}H]estradiol (retention times = 33 and 34 min), revealed, respectively, two overlapping subcleaved fragments 25−35, A−S−G−N−I−H−N−(*X)−L−A−(W), and 25−36, A−S−G−N−I−H−N−(*X)−L−A−(W)−Y, both derived from the tryptic peptide 25−39 (Table 2). The C-terminal chymotryptic subcleavages after TrpL-35 and TyrL-36, respectively, may be due to a partial degradation of TPCK-trypsin as mentioned above. The shorter peptide has been assigned as the fragment 25−35 rather than the fragment 25−34, owing to the parallel absence of TrpL-35 residue in the complete sequence of peptide 25−36 and to the low probability of a chymotryptic subcleavage after an alanine residue, as a side-reaction after direct treatment by trypsin. For these two peptides, no known amino acid residues could be identified at the 8th and 11th Edman cycles corresponding to TyrL-32 and TrpL-35, respectively. The radioactivity profile, measured only for peptide 25−36, showed that a major peak of radioactivity (Table 2) was eluted exclusively at the 8th cycle and corresponded in magnitude with the amounts of PTH derivatives measured at the preceding cycle, thus confirming a specific labeling of TyrL-32 residue. The absence of detectable TrpL-35 residue in both peptides 25−35 and 25−36, as already observed after photolabeling with 3-ANBA-EA-carboxymethyloxy-[17α-^{3}H]estradiol, also led to further characterizations by mass spectrometry which were successful only for the labeled peptide 25−36, but not for the shorter peptide 25−35 which failed to give any detectable signal (vide infra).

The major radioactive tryptic peptide of L chain photolabeled with 6β-ANBA-[17α-^{3}H]estradiol was found to correspond to the intact tryptic fragment 25−39, A−S−G−N−I−H−N−(*X)−L−A−W−Y−Q−Q−K, in which the TyrL-32 residue was absent at the 8th Edman cycle while the main peak of radioactivity was eluted at this same cycle, indicating unambiguously that TyrL-32 is the major site of photolabeling (Table 3).

The major tryptic peptide of the H chain photolabeled with 6β-ANBA-[17α-^{3}H]estradiol was identified as the fragment 41−54, P−G−Q−G−L−E−W−I−G−(*X)−L−D−P−Y,

Table 3: Amino Acid Sequence Analysis of L and H Chain Tryptic Peptides Photolabeled with 6β-ANBA-Estradiol

		6β-ANBA-estradiol-peptides L chain				6β-ANBA-estradiol-peptides H chain	
		peptide 25−39 L (85 995 dpm) 564 pmol[a]				peptide 41−54 H (36 335 dpm) 238 pmol[a]	
cycle no.	amino acid	PTH derivative (pmol)	radioactivity (dpm)	cycle no.	amino acid	PTH derivative (pmol)	radioactivity (dpm)
1	A	245	2370	1	P	217	1330
2	S	38	2190	2	G	142	2268
3	G	162	2097	3	Q	268	2397
4	N	158	1952	4	G	86	1998
5	I	152	2128	5	L	138	1974
6	H	61	2209	6	E	88	1500
7	N	138	1632	7	W	35	1858
8	Y	105[b]	15 980	8	I	95	1319
9	L	138	7261	9	G	73	861
10	A	119	4782	10	Y	56[b]	8491
11	W	25	3375	11	L	98	3913
12	Y	99	2767	12	D	74	2061
13	Q	92	2069	13	P	59	1515
14	Q	nq[c]	2211	14	Y	39	1375
15	K	38	2131	15			1015
16			1632	16			1113
17			1512	17			731
18			2003	18			850
filter			14 218	filter			13 420

[a] Picomoles of labeled peptide applied to the sequencer calculated from the specific activity of the corresponding radioactive photoreagent. [b] Picomoles of labeled amino acid estimated from the radioactivity eluted at this Edman cycle (no PTH derivative of the unlabeled amino acid was detected at this cycle). [c] Not quantified.

resulting from C-terminal chymotryptic subcleavage of tryptic peptide 41−59 (Table 3). No known amino acid could be detected at the 10th Edman cycle while the major peak of radioactivity was also recovered at this cycle, thus demonstrating that the corresponding TyrH-50 is the site of photoaffinity-labeling. A minor radioactive HPLC fraction (retention time = 35−38 min) was also sequenced and was found to contain a longer photolabeled tryptic peptide 39−59, for which the elution of the radioactivity was observed at the 12th Edman cycle corresponding to the same Y-50 H residue (data not shown).

The major radioactive tryptic peptide of the L chain photolabeled with 7-ANBA-EA-CMO-[17α-^{3}H]estradiol (retention time = 31 min) was found to correspond to the fragment 25−35, A−S−G−N−I−H−N−(*X)−L−A−(W) (Table 4) in which the Trp-35 could not be identified, rather than to the shorter peptide 25−34, as discussed above for the 6α-ANBA-estradiol photoreagent. This hypothesis was confirmed unambiguously by complementary mass spectrometry studies (vide infra). For the peptide 25−35 photolabeled with 7-ANBA-EA-CMO-[17α-^{3}H]estradiol, no detectable PTH derivative was present at the 8th Edman cycle, which was also found to correspond to a small peak of radioactivity, in agreement with, at least, a partial labeling of the TyrL-32 residue. As expected for this photolabeled peptide, which had also been found to be rapidly hydrolyzed in the acidic conditions of HPLC purification, the bulk of radioactivity was eluted at the first Edman cycle, corresponding to an intact AlaL-25 residue which is a highly improbable site of labeling for aryl azides. The total absence of TyrL-32 suggests that this residue is the site of labile covalent labeling with 7-ANBA-EA-CMO-estradiol, in agreement with the fact that tyrosine is expected to be a preferential target for aryl azide photoreagents. The absence of TrpL-35 residue also suggests that this amino acid may be another potential site of labeling, but such a hypothesis has been considered to be rather improbable, by analogy with the parallel absence of TrpL-35 in the two peptides 25−35 and 25−36 photolabeled with 6α-ANBA-[17α-^{3}H]estradiol, for which the covalent labeling was more stable and afforded a major peak of radioactivity unambiguously located on the TyrL-32 residue.

Table 4: Amino Acid Sequence Analysis of L Chain Peptides Photolabeled with 7-ANBA-EA-CMO-Estradiol

		7-ANBA-EA-CMO-estradiol-peptides			
		peptide 25−35 L (91 564 dpm) 238 pmol[a]		peptide 25−39 L (27 830 dpm) 89 pmol[a]	
cycle no.	amino acid	PTH derivative pmol	radio-activity dpm	PTH derivative pmol	radio-activity dpm
1	A	74	46 508	44	556
2	S	26	12 820	9	224
3	G	72	3290	21	117
4	N	51	1771	24	105
5	I	62	1270	22	69
6	H	38	938	11	48
7	N	52	861	19	59
8	Y	3[b]	1165	0.3[b]	102
9	L	32	1022	17	73
10	A	17	885	13	73
11	W	nd[c]	700	nd[c]	75
12	Y		724	8	62
13	Q		1568	10	64
14	Q		430	nq[d]	45
15	K		395	4	61
filter			5326		850

[a] Picomoles of labeled peptide applied to the sequencer calculated from the specific activity of the corresponding radioactive photoreagent. [b] Picomoles of labeled amino acid estimated from the radioactivity eluted at this Edman cycle (no PTH derivative of the unlabeled amino acid was detected at this cycle). [c] Not determined (no corresponding PTH derivative was detected at this cycle). [d] Not quantified.

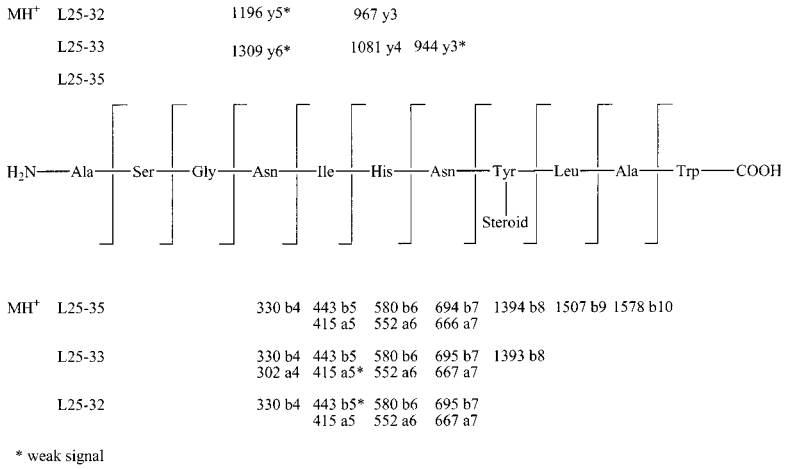

FIGURE 6: Fragmentation scheme corresponding to the PSD-MALDI-TOF fragmentations of the three overlapping peptides 25−35, 25−33, and 25−32 of L chain photolabeled with 3-ANBA-EA-carboxymethylestradiol.

The minor peak of L chain photolabeled with 7-ANBA-EA-CMO-[17α-^{3}H]estradiol (retention time = 32 min) could be only partially characterized by the sequence of the first four N-terminal residues A−S−G−N and was postulated to correspond to a labeled peptide fragment 25−36, homologous to the fully characterized peptide 25−36 photolabeled with 6α-ANBA-[17α-^{3}H]estradiol, owing to the similar differences in retention times. The other minor peak of L chain photolabeled with 7-ANBA-EA-CMO-[17α-^{3}H]estradiol (retention time = 26 min) was characterized as the tryptic peptide 25−39 in which both TyrL-32 and TrpL-35 residues were absent in the Edman sequence while a very small radioactive peak was present only at the level of TyrL-32 (Table 4).

Mass Spectrometry. Direct evidence for the presence of covalently attached steroid photolabels was provided by determination of molecular masses of steroid−peptide conjugates by mass spectrometry.

MALDI-TOF mass spectrometry (linear mode) of the sequenced major peptide fragment 25−35 of L chain photolabeled with 3-ANBA-EA-carboxymethyloxy-[17α-^{3}H]-estradiol, purified by HPLC, showed a $[M + H]^+$ ion at *m*/*z* 1779.8, corresponding to the calculated isotopic mass, $M = 1778.8$, obtained after covalent addition of 1 mol of nitrene photoreagent. The two corresponding photolabeled peptides obtained after chymotryptic subcleavage, also purified by HPLC, failed to give any interpretable mass spectra. Therefore, MALDI-TOF mass spectrometry was performed directly on the immunopurified mixture of photolabeled peptides obtained after two successive tryptic and chymotryptic cleavages. A predominant $[M + H]^+$ ion signal was observed at 1522.7, corresponding to the calculated mass, $M = 1521.7$, of the peptide fragment 25−33 of L chain covalently labeled with 1 mol of nitrene photoreagent, while a less intense signal was found at 1409.7, assigned to the photolabeled subcleaved 25−32 fragment (calculated mass, $M = 1408.6$). A minor peak was also observed at 1779.8, which might correspond to a residual amount of uncleaved photolabeled peptide 25−35. The peptide fragment 25−33 corresponds to a C-terminal chymotryptic subcleavage after leucine, a known minor site for chymotrypsin. The presence of the photolabel on peptide 25−32 indicates that covalent labeling with 3-ANBA-EA-carboxymethyloxyestradiol cannot be located beyond TyrL-32. The PSD spectra recorded for the three photolabeled peptide fragments 25−32, 25−33, and 25−35 (Figure 6) exhibited mostly a and b ion signals, whereas few y signals could be observed. A b/y ion correspondence was detected for b5/y3 of peptide 25−32 (weak b5 signal) or b6/y3 of peptide 25−35 (weak y3 signal) and unambiguously established for b5/y4 of peptide 25−33 (two intense signals), excluding the presence of the photolabel before AsnL-31. Therefore, only AsnL-31 and TyrL-32 remained as potential targets of photolabeling. In the absence of b/y diagnostic ion pairs at the level of these two residues, inspection of a and b ion signals of the three peptides showed, in all cases, mass values for the a7 and b7 fragments (cleaved after Asn-31), totally incompatible with the presence of photolabel on this residue. Finally, direct evidence for the photolabeling of the remaining TyrL-32 was provided by the presence of b8 fragments (cleaved after TyrL-32) for both peptides 25−33 and 25−35, with mass values consistent with the addition of 1 mol of nitrene photoreagent on this residue.

Electrospray ionization mass spectrometry of the peptide 25−36 of the L chain photolabeled with 6α-ANBA-[17α-^{3}H]estradiol showed a major characteristic protonated ion appearing at 929.8, identified as the $[M + 2H]^{2+}$ ion corresponding to the calculated isotopic mass, $M = 1857.9$, of the peptide fragment 25−36, A−S−G−N−I−H−N−(*Y)−L−A−W−Y, photolabeled with 1 mol of the nitrene derivative of the 6α-ANBA photoreagent. Two other weak protonated ions were observed either at 1858.8 ($[M + H]^+$) or at 620.0 ($[M + 3H]^{3+}$), according to experimental conditions. The other major peptide 25−35 photolabeled with 6α-ANBA-[17α-^{3}H]estradiol failed to give interpretable mass spectra.

Electrospray ionization mass spectrometry of the peptide 25−39 of the L chain photolabeled with 6β-ANBA-estradiol showed two characteristic protonated ions, $[M + 2H]^{2+}$ and $[M + 3H]^{3+}$ at 1122.2 and 748.5, respectively, corresponding to the calculated mass, $M = 2242.1$, of the L chain tryptic peptide, A−S−G−N−I−H−N−(*Y)−L−A−W−Y−Q−Q−K, photolabeled with 1 mol of the nitrene derivative of the 6β-ANBA-estradiol photoreagent. An intense signal was also found at 987 and was tentatively assigned to the $[M + 2H]^{2+}$ ion corresponding to the loss of Δ^6-estradiol. The covalent binding of the photoreagent on peptide 25−39 was also confirmed by LSIMS which revealed a $[M + H]^+$

ion at 2242.7 as well as the two corresponding $[M + Na]^+$ and $[M + K]^+$ ions.

Electrospray ionization mass spectrometry of the peptide 41−54 of the H chain photolabeled with 6β-ANBA-[17α-^{3}H]estradiol showed a protonated $[M + 2H]^{2+}$ ion at 1029.8, as the major signal, corresponding to the calculated isotopic mass, $M = 2057.0$, of the H chain peptide fragment, P−G−Q−G−L−E−W−I−G−(*Y)−L−D−P−Y, photolabeled with 1 mol of the nitrene derivative of the 6β-ANBA photoreagent. This result was also corroborated by LSIMS which showed the $[M + H]^+$ ion at 2057.4, as well as the corresponding $[M + Na]^+$ and $[M + K]^+$ ions, thus confirming the covalent character of the photoadduct.

For the labeling with 7-ANBA-EA-CMO-estradiol derivative, it was extremely difficult to isolate an intact peptide-steroid photoadduct, due to the instability of the covalent link in acidic conditions of HPLC purification, as shown by the rapid and progressive decomposition of the purified radioactive conjugate in successive HPLC steps. Such a hydrolysis was presumed to occur at the level of the acid-labile CMO bond. Attempts to identify extemporaneously this photoadduct have been made by combined liquid chromatography-electrospray mass spectrometry which revealed only a very small amount of intact photolabeled peptide characterized by a major $[M + 2H]^{2+}$ ion at 1179.4, corresponding to the calculated isotopic mass, $M = 2355.1$ after addition of 1 mol of steroid nitrene on the tryptic peptide 25−39 of the L chain. No signal corresponding to acid cleavage of the CMO link of the photolabel could be found. Therefore, to circumvent these difficulties, inherent to the HPLC separation step, MALDI-TOF mass spectrometry was performed directly on the mixture of labeled tryptic peptides eluted after immunoaffinity. Two major peaks were observed at 1808.4/1809.4 and 1830.4, assigned, respectively, to the $[M + H]^+$ and $[M + Na]^+$ ions of L chain peptide fragment 25−35, A−S−G−N−I−H−N−(*Y)−L−A−W, labeled with 1 mol of the nitrene derivative of the 7-ANBA-EA-CMO-estradiol photoreagent (calculated isotopic mass, $M =$ 1807.6). A less intense peak was also observed at 1438.4, assigned to its subcleaved photolabeled fragment 25−32 (calculated isotopic mass, $M = 1437.6$), but no peak corresponding to the intact photolabeled tryptic peptide fragment 25−39 was present. These findings are in keeping with the presence of a labeled peptide fragment 25−35 rather than of the shorter peptide 25−34 and confirm that covalent photoaffinity-labeling has occurred, most probably at the level of TyrL-32 given the absence of any detectable PTH derivative of tyrosine in Edman degradation of peptide 25−35. However, the presence of a photolabeled fragment 25−32, as revealed by mass spectrometry, shows that photolabeling at the level of TyrL-32 does not seem to inhibit chymotryptic subcleavage after this residue, as observed above after labeling with 3-ANBA-EA-carboxymethyloxy-estradiol.

DISCUSSION

The monoclonal anti-7-CMO estradiol antibody 9D3 has an overall similarity to the previously reported anti-6-CMO-estradiol antibody 57-2 (*1*) which also exhibits a preferred recognition of D-ring of estradiol, confirmed by the results of molecular modeling. Although cross-reactions of antibody 9D3 with estradiol 3-sulfate and 3-glucuronide are significantly higher (51 and 28%, respectively) than those of antibody 57-2 (7 and 23%), the cross-reaction of antibody 9D3 with testosterone is very low (0.1%), in contrast to that found for antibody 57-2 (37%), a feature possibly due to the conjugation of the 6-CMO link with the aromatic A-ring of estradiol which may alter the recognition of the phenolic group by antibody 57-2. Besides the higher affinity of antibody 9D3 for estradiol ($K_a = 1.3 \times 10^{10}$ M^{-1} at 4 °C) than reported for antibody 57-2 ($K_a = 3.9 \times 10^8$ M^{-1}) (*21*), the most salient difference between these two antibodies is the cross-reactivity of anti-7-CMO-estradiol antibody 9D3 with both 6- and 7-substituted derivatives of estradiol (highest corresponding cross-reactions observed for 6-ANBA-EA-CMO-estradiol = 160% and for the 7-ANBA-EA-CMO-estradiol = 110%) which appears rather modest, as compared with the huge cross-reactivity of anti-6-CMO-estradiol antibody 57-2 with 6-derivatives (from 356%, for 6ξ-hydroxyestradiol to 1393%, for the 6-CMO-estradiol hapten). On the other hand, antibody 57-2 has only a very low cross-reaction with the single tested 7-derivative, 7α-methylestradiol (0.65%).

Affinity-labeling experiments were designed to provide direct evidence concerning the positioning of the steroid inside the combining binding site of antibody 9D3, with the view of refining molecular modeling of the steroid-antibody complex, a major prerequisite step before undertaking modifications by antibody engineering technologies. The difficulties which may be encountered for molecular modeling of a steroid-antibody complex are illustrated by the recent three-dimensional structures of Fab′−steroid complexes of anti-progesterone antibody DB3, which have demonstrated that its combining site binds substituted progesterone derivatives or 5β-H-dihydroprogesterone and etiocholanone analogues in two opposite orientations (*40*). Therefore, the possibility that the combining sites of other anti-steroid antibodies may also accommodate opposite orientations of steroid derivatives according to their structures has to be considered for the design of appropriate regiospecific modifications in order to improve binding specificity. Useful experimental information on the stereochemistry of insertion of these structures in the antibody combining site can be obtained from affinity-labeling studies which reflect steroid-antibody interactions in solution.

The general purpose of this work was to find affinity-labeling probes for anti-estradiol antibody 9D3, having a capacity to reach the poorly specific domains of the antibody combining site encompassing C3, C6, and C7 positions of estradiol, which are the main targets for antibody reshaping, especially around the C3 position. The identification in these domains of affinity-labeled residues is particularly useful for improving the docking of the steroid in the molecular modeling of these loose regions of the site, which is expected to be more difficult than for the specific contact regions with the steroid hapten. Affinity-labeling experiments were undertaken with five estradiol photoreagents sharing a same photoactivable azidonitrobenzoylamido chromophore coupled at the extremity of a 3-aminoethyloxy- or 3-aminoethyl-amidomethyloxy spacer arm or on a 6α- or 6β-amino group, and at the extremity of an aminoethylamido spacer arm introduced on the 7-CMO-estradiol hapten link. Although photolysis of the photoreagent alone was very rapid, much

longer irradiation times have been employed for preparative photolabeling in order to improve the yields. However, preliminary analytical experiments have been made in order to verify that the increase in yield does not result from the formation of sites of labeling different from those obtained after short irradiation times. For all photoreagents, the TrpL-35 residue was either recovered in very low yield (C3 derivatives) or absent in the Edman sequence. Presumably, the TrpL-35 was nonspecifically denatured by storage and/or experimental conditions of Edman sequencing but not of mass spectrometry. In all cases the covalent character of photolabeling was established by mass spectrometry, which showed a stoichiometry of 1 mol of label/mol of peptide and confirmed the presence of tryptophan.

The first objective of this study was to determine whether a loose region of the combining site of antibody 9D3 is still present around the solvent-exposed 3-phenolic group and has a size sufficient to explain the lack of specificity for the C3 position, as reflected by the relatively high cross-reactions with estradiol 3-sulfate and 3-glucuronide. The short 3-ANBA-ethyloxyestradiol derivative exhibited a high cross-reaction (93%) but failed to give any significant photolabeling. Only the long 3-ANBA-ethylamidocarboxymethyloxyestradiol derivative, showing also a similarly high cross-reactivity (106%), led to a specific covalent labeling mostly recovered on L chain, at the level of TyrL-32. The absence of labeling with the short 3-ANBA-ethyloxyestradiol photoreagent suggests that the size of the side-chain is probably critical for obtaining an interaction of the ANBA chromophore with an amino acid target. The labeling of TyrL-32 on the CDR L1 loop, as well as the absence of photolabeling with the shorter C3 derivative, which points to the presence of a large subsite around the C3 position, provides information that would be particularly useful for improving the specificity of the 9D3 antibody for the 3-phenolic A-ring part of estradiol. Genetic engineering modifications have already been reported in the case of the anti-estradiol antibody 57-2, by lengthening of the CDR H2 loop, which was found to inhibit the large cross-reactivity of this antibody with testosterone and to improve significantly its binding affinities for estradiol as well as for 4- and 6-biotinylated estradiol panning derivatives (*2*). A potential advantage of the anti-7-CMO estradiol antibody 9D3, as compared with the anti-6-CMO estradiol antibody 57-2, is the greater distance between the C3 position and the CMO group which might allow more substantial modifications of the combining site to be made around the C3 position, without inducing simultaneously too severe changes in the recognition of the hapten link.

The second objective of this work was to determine the most proximal amino acid residues in the vicinity of the C6 position of estradiol in order to explain the lack of specificity of antibody 9D3 for the C6 position which is, however, less pronounced than reported for the anti-6-CMO estradiol antibody 57-2 (*1*). Affinity-labeling experiments were undertaken with the two 6α- and 6*β*-ANBA-[^{3}H]estradiol photoreagents, previously reported as photoaffinity-labeling reagents of the anti-7-CMO-estradiol antibody 15H11 (*16*). The 6α-ANBA-estradiol photoreagent was found to label exclusively the L chain whereas the 6*β*-epimer labeled both the L and H chains (70 and 30% of the amount of total labeling, respectively). The less-*cross*-reactive 6*β*-ANBA derivative led to a significantly higher labeling yield than the 6α-epimer, owing probably to a more appropriate geometry of interaction between the 6*β*-ANBA chromophore and its two target amino acids on L and H chains. After enzymatic cleavage with TPCK-trypsin, the 6α-ANBA derivative was localized at the level of the TyrL-32 residue, on two overlapping peptide fragments 25−35 and 25−36 resulting, respectively, from chymotryptic subcleavages after TrpL-35 and TyrL-36 at the C-terminal end of the tryptic peptide 25−39. The fraction of 6*β*-ANBA derivative present on the L chain was recovered on the intact tryptic peptide 25−39, at the level of the same TyrL-32 residue as the one labeled by the 6α-epimer. The absence of chymotryptic subcleavage only for the peptide labeled with the 6*β*-ANBA epimer, had also been previously observed for the photolabeling of 15H11 antibody (*16*). The fraction of 6*β*-ANBA derivative present on the H chain was recovered predominantly on the peptide fragment 41−54 resulting from a C-terminal chymotryptic subcleavage of the tryptic peptide 41−59 after TyrH-54 and was localized exclusively at the level of TyrH-50. The higher cross-reactivity of the equatorial 6α-ANBA-estradiol derivative (103%), as compared with that of the axial 6*β*-epimer (33%), and the labeling of TyrH-50 by the 6*β*-epimer, only, suggest that the binding domain around the C6 position exerts asymmetrical steric constraints, presumably beyond a minimal distance from C6 position, since much smaller 6α- and 6*β*-bromoacetamidoestradiol epimers were found to exhibit only a slight difference of cross-reactivity (20 and 15%, respectively). The existence of two simultaneous sites of photolabeling with the same 6*β*-derivative at TyrL-32 and TyrH-50 indicates that these two amino acids are both within reach of the extremity of the ANBA photoreagent. Attempts have been made to employ 6α- and 6*β*-bromoacetamidoestradiol chemoaffinity reagents but these two compounds failed to induce covalent labeling (data not shown).

The third objective was to map the subsite of antibody 9D3 corresponding to the 7-CMO hapten link, to determine whether the extremity of the CMO bond is still localized in a subsite corresponding to the hapten link or emerged in the solvent. Such information is of prime importance for the design of steroid tracers, i.e., those coupled to enzyme labels, which may be sensitive to steric constraints. The 7-ANBA-EA-CMO-estradiol photoreagent formed a covalent adduct almost totally recovered on the L chain. Only a very small fraction was observed on the H chain and was not further analyzed. The 7-ANBA-EA-CMO-estradiol photoreagent was localized at the level of TyrL-32, as found with the two 6α- and 6*β*-ANBA-estradiol derivatives. This indicates that the relatively rigid and short 7-CMO-estradiol link of the hapten is probably inserted in a wide binding pocket which can accommodate both 6- and 7-substituents. In a paradoxical manner for an anti-7-CMO-estradiol antibody, 7-ANBA-EA-CMO-estradiol was less cross-reactive (110%) than the 6-ANBA-EA-CMO-estradiol isomer (160%). This part of the binding site is probably different from the corresponding region of the anti-6-CMO-estradiol antibody 57-2, which exhibits much higher cross-reactions with 6-substituents (356−1393%) but a low cross-reaction with the only tested 7-substituted steroid, 7α-methylestradiol.

The photoaffinity-labeling of the same TyrL-32 residue by 3-ANBA-EA-carboxymethyloxyestradiol, 6α- or 6*β*-ANBA-estradiol, and 7-ANBA-EA-CMO-estradiol photo-

reagents indicates that, in all four cases, TyrL-32 is within reach of the azide group and that C3, C6, and C7 positions remain inserted in a large subsite without barrier between the domains encompassing each of these three positions. However, the stability of the photoadducts on TyrL-32 in the acidic conditions of Edman degradation, as revealed by comparing the fraction of radioactivity released at the corresponding cycle with the radioactivity observed at the preceding cycles, varied according to the side-chain structure of the photoreagent. Labeling of TyrL-32 with 3-ANBA-EA-carboxymethyloxyestradiol, 6α-ANBA-estradiol, and 6*β*-ANBA-estradiol was stable while labeling with 7-ANBA-EA-CMO-estradiol was almost totally labile, possibly due to the hydrolysis of the acid-labile 7-oxime link. The photoaffinity-labeling of the same TyrL-32 amino acid by all C3-, C6-, and C7-substituted ANBA photoreagents employed in this study confirms that tyrosine residues, often reported as sites of photolabeling for aryl azide chromophores (*41*), represent preferential targets for 5-azido-2-nitrobenzoyl-amido chromophores as long as an interaction remains possible, due to conformational mobility of the chromophore and/or of the intermediate link. One may speculate whether such an interaction may contribute to the high cross-reactivity of the ANBA photoreagents observed in this work. In the very recently published crystal structure of antibody 57-2 determined in the presence of estradiol (*42*), TyrL-32, located on the CDR L1 loop, is not mentioned among contact residues with estradiol. On the other hand, the TyrH-50 residue of the CDR H2 loop of antibody 9D3, identified by photolabeling with 6*β*-ANBA-estradiol, belongs to the group of frequent contact amino acids of anti-hapten antibodies (*43*). These observations are consistent with structural data obtained from two alternative preliminary molecular models of the interaction of estradiol with the antibody 9D3 combining site (Coulon, S., et al., unpublished results) in which a steroid can be docked according to two possible orientations, differing by rotation around the 17-OH extremity, one with the A-ring inserted between H2 and L3 loops, as predicted in a previous model of the anti-estradiol antibody 57-2 of similar specificity profile (*1*), and the other one with A-ring inserted between H3 and L2 loops, as strongly suggested by the crystal structure of antibody 57-2 (*42*). In both models, TyrH-50, photolabeled only by the 6*β*-ANBA photoreagent, is located on the *β*-face of estradiol. On the other hand, TyrL-32, photolabeled by both 6α- and 6*β*-ANBA epimers as well as by the two other C3- and C7-linked photoreagents, is located on the *β*-face of estradiol, in the first model, or on the α-face, in the second model, which is slightly more consistent with the labeling of TyrL-32 only by 6α-ANBA photoreagents. Further refinements of these structural models and complementary affinity-labeling experiments are in progress in the view of determining whether one of these two potential orientations of estradiol could indeed be more compatible with the affinity-labeling results.

These findings open the way to modify the combining site of the anti-7-CMO-estradiol 9D3 antibody by genetic engineering in order to improve its specificity, mainly for the C3 and C6 positions, while the cross-reactivity of this antibody with both C6 and C7 positions may facilitate the concomitant selection of mutants having a binding site able to accommodate a modified steroid tracer bearing a side chain either at C6 or C7 position, more stable than the acid-labile 7-CMO group of the haptenic steroid.

ACKNOWLEDGMENT

The authors are particularly indebted to M. Courteau, and D. Mazzocut (IBCP-CNRS, Lyon, France) for sequence determinations, to M. Becchi, M. M. Flament, O. Pais, C. Chambon (Centre Commun de Spectrométrie de Masse, CNRS, Lyon-Solaize, France), to J. Bonicel (IBSM, CNRS, Marseille, France), to D. Bouchu and L. Rousset (ESCPE, Université Claude Bernard, Villeurbanne, France), to T. Kalgar-Grisel (Waters Application Laboratory, Courtaboeuf, France), for mass spectra, and to B. Fenet and O. Miani (ESCPE, University Claude Bernard, Villeurbanne, France) for NMR spectra. Thanks are also due to J. Hoebeke (IBMC, CNRS, Strasbourg, France) and to J.-L. Pellequer (CEA, Bagnois-sur-Cèze, France) for helpful discussions, M. Ainouze for technical assistance, and to J. Carew for help in editing the manuscript.

SUPPORTING INFORMATION AVAILABLE

Figures showing the HPLC profiles of immunopurified peptides from tryptic digests of antibody 9D3 photolabeled with C3-, C6-, or C7-linked ANBA derivatives of estradiol and the mass spectra of photolabeled peptides. This material is available free of charge via the Internet at http://pubs.acs.org.

REFERENCES

1. Lamminmäki, U., Villoutreix, B. O., Jauria, P., Saviranta, P., Vihinen, M., Nilsson, L., Teleman, O., and Lövgren, T. (1997) *Mol. Immunol. 34*, 1215−1226.
2. Saviranta, P., Pajunen, M., Jauria, P., Karp, M., Pettersson, K., Mäntsälä, P., and Lövgren, T. (1998) *Protein Eng. 11*, 143−52.
3. Barnard, G. J. R., Hennam, J. F., and Collins, W. P. (1975) *J. Steroid Biochem. 6*, 107−116.
4. Kim J. B., Barnard, G. J., Collins, W. P., Kohen, F., Lindner, H. R., and Eshhar, Z. (1982) *Clin. Chem. 28*, 1120−1124.
5. Mandal, C., and Ali, N. (1988) *Steroids 52*, 551−560.
6. De Boever, J., Kohen, F., Bouve, J., Leyseele D., and Vandekerckhove, D. (1990) *Clin. Chem. 36*, 2036−2041.
7. De Lauzon, S., Desfosses, B., Christeff, N., Hanquez, C., and Cittanova, N. (1992) *J. Steroid Biochem. Mol. Biol. 42*, 223−228.
8. England, B. G., Niswender, G. D., and Midgley, A. R., Jr. (1974) *J. Clin. Endocrinol. Metab. 38*, 42−50.
9. Rao, P. N., Moore, P. H., Jr., Somawardhana, C. W., and Guajardo, R. J. (1990) *Clin. Chem. 36*, 1099.
10. Fantl, V. E., and Wang D. Y. (1984) *J. Endocr. 100*, 367−376.
11. De Lauzon, S., Desfosses, B., Moreau, M.-F., Le Trang, N., Rajkowski, K., and Cittanova, N. (1990) *Hybridoma 9*, 481−491.
12. Agasan, A. L., Briggs, M. H., Hewish, D. R., and Stewart, B. (1986) *Steroids 47*, 295−306.
13. Bettsworth, F., Monnet, C., Watelet, B., Battail-Poirot, N., Gilquin, B., Jolivet, M., Menez, A., Arnaud, M., and Ducancel, F. (2001) *J. Mol. Recognit. 14*, 99−109.
14. Franek, M. (1987) *J. Steroid Biochem. 28*, 95−108.
15. Mappus, E., Grenot, C., Forest, M., and Cuilleron, C. Y. (1975) *C. R. Acad. Sci. Paris, Ser. C 281*, 247−250.
16. Rousselot, P., Mappus, E., Blachère, T., Rolland de Ravel, M., Grenot, C., Tonnelle, C., and Cuilleron, C. Y. (1997) *Biochemistry 36*, 7860−7868.

17. Jackson, T., Morris, B. A., Martin, A. C. R., Lewis, D. F. V., and Sanders, P. (1992) *Protein Eng. 5*, 343−50.
18. Schildbach, J. F., Near, R. I., Parks, D. R., Bruccoleri, R. E., Haber, E., Jeffrey, P. D., Shi-Chung, Ng., Novotny, J., Sheriff, S., and Margolies, M. N. (1993) *J. Biol. Chem. 268*, 21739−21747.
19. Ping, J., Schildbach, J. F., Shaw, S.-Y, Quertermous, T., Novotny, J., Bruccoleri, R. E., and Margolies, M. N. (1993) *J. Biol. Chem. 268*, 23000−23007.
20. Chames, P., Coulon, S., and Baty, D. (1998) *J. Immunol. 161*, 5421−5429
21. Lamminmäki, U., Pauperio, S., Westerlund-Karlson, A., Karvinen, J., Virtanen, P. L., Lövgren, T., and Saviranta, P. (1999) *J. Mol. Biol. 291*, 589−602.
22. Ehrenstorfer-Schaefers, E.-M., Steiner, N., and Altman, J. (1990) *Naturforsch. B 45*, 817−827.
23. Rao, P. N., and Moore, P. H., Jr. (1977) *Steroids 29*, 461−469.
24. Dhar, T. K., Samanta, A. K., and Ali, E. (1988) *Steroids 51*, 519−525.
25. Torelli, V., and Pierdet, A. (Roussel-UCLAF) (1975) *Ger. Offen.* 2,429,040 (Chem. Abstr. 82: 140387z).
26. Bowden, K., Heilbron, I. M., Jones, E. R. H., and Weedon, B. C. L. (1946) *J. Chem. Soc.* 39−45.
27. Tillman, D. M., Jou, N. T., and Marion, T. N. (1992) *J. Exp. Med. 176*, 761−779.
28. Retter, M. W., Cohen, P. L., Eisenberg, R. A., and Clarke, S. H. (1996) *J. Immunol. 156*, 1296−1306.
29. Pajunen, M., Saviranta, P., Jauria, P., Karp, M., Pettersson, K., Mäntsälä, P., and Lövgren, T. (1997) *Biochim. Biophys. Acta 1351*, 192−202.
30. Carbone, F. R., and Paterson, Y. (1985) *J. Immunol. 135*, 2609−2616.
31. Mylvaganam, S. E., Paterson, Y., Kaiser, K., Bowdish, K., and Getzoff, E. D. (1991) *J. Mol. Biol. 221*, 455−462.
32. Kabat, E. A., Wu, T. T., Reid-Muller, M., Perry, H. M., and Gottesman, K. S. (1987) *Sequences of Proteins of Immunological Interest*, 4th ed., U.S. Department of Health and Human Services, Public Health Service, National Institute of Health, Bethesda, MD.
33. Chothia, C., and Lesk, A. M. (1987) *J. Mol. Biol. 196*, 901−917.
34. Taylor, C. A. Jr., Smith, H. E., and Danzo, B. J. (1980) *Proc. Natl. Acad. Sci. U.S.A. 77*, 234−238.
35. Grenot, C., de Montard, A., Blachère, T., Rolland de Ravel, M., Mappus, E., and Cuilleron, C. Y. (1992) *Biochemistry 31*, 7609−7621.
36. Grenot, C., Blachère, T., Rolland de Ravel, M., Mappus, E., and Cuilleron, C. Y. (1994) *Biochemistry 33*, 8969−8981.
37. Wilchek, M., Bocchini, V., Becker, M., and Givol, D. (1971) *Biochemistry 10*, 2828−2834.
38. Smith, R. L., and Shaw, E. (1969) *J. Biol. Chem. 244*, 4704−4712.
39. Keil-Dlouha, V., and Zybler, N., Imhoff, J.-M., Tong, N.-T., Keil, B. (1971) *FEBS Lett. 16*, 291−295.
40. Arevalo, J. H., Hassig, C. A., Stura, E. A., Sims, M. J., Taussig, M. J., and Wilson, I. A. (1994) *J. Mol. Biol. 241*, 663−690.
41. Kotzyba-Hibert, F., Kapfer, I., and Goeldner, M. (1995) *Angew. Chem., Int. Ed. Engl. 34*, 1296−1312.
42. Lamminmäki, U., and Kankare, J. A. (2001) *J. Biol. Chem. 276*, 36687−36694.
43. MacCallum, R. M., Martin, A. C., and Thornton, J. M. (1996) *J. Mol. Biol. 262*, 732−745.

BI011174B